LU TP 15-51
November 2015

Dynamic colour screening in diffractive deep inelastic scattering

Gunnar Ingelman,[1,*] Roman Pasechnik,[2,†] and Dominik Werder[1,‡]

[1] *Department of Physics and Astronomy, Uppsala University, Box 516, 75120 Uppsala, Sweden*

[2] *Department of Astronomy and Theoretical Physics, Lund University, 22362 Lund, Sweden*

Abstract

We present a novel Monte-Carlo implementation of dynamic colour screening via multiple exchanges of semi-soft gluons as a basic QCD mechanism to understand diffractive electron-proton scattering at the HERA collider. Based on the kinematics of individual events in the standard QCD description of deep inelastic scattering at the parton level, which at low x is dominantly gluon-initiated, the probability is evaluated for additional exchanges of softer gluons resulting in an overall colour singlet exchange leading to a forward proton and a rapidity gap as the characteristic observables for diffractive scattering. The probability depends on the impact parameter of the soft exchanges and varies with the transverse size of the hard scattering subsystem and is therefore influenced by different QCD effects. We account for matrix elements and parton shower evolution either via conventional DGLAP $\log Q^2$-evolution with collinear factorisation or CCFM small-x evolution with $k_\perp$-factorisation and discuss the sensitivity to the gluon density distribution in the proton and the importance of large $\log x$-contributions. The overall result is that, with only two model parameters which have theoretically motivated values, a satisfactory description of the observed diffractive cross-section at HERA is obtained in a wide kinematical range.

* Gunnar.Ingelman@physics.uu.se

† Roman.Pasechnik@thep.lu.se

‡ Dominik.Werder@physics.uu.se

I. INTRODUCTION

Diffractive scattering through strong interactions without any large momentum transfer has historically been described in terms of the exchange of a Pomeron, a virtual hadron-like object with vacuum quantum numbers. The Regge approach [1, 2] of the pre-QCD era provides a working phenomenology to describe such processes in a hadron basis since no parton structure is resolved. The idea [3] to introduce a hard scale in a diffractive process opened the possibility to examine these processes at the level of quarks and gluons in the modern framework of QCD. The discovery of such *diffractive hard scattering* was made by the UA8 experiment [4] by observing high-$p_\perp$ jets in single diffractive events in $p\bar{p}$ collisions at CERN. Many other hard processes in diffractive events have been observed later on, for a review see e.g. [5]. Of special importance are the measurements of diffractive deep inelastic scattering (DDIS) at the electron-proton collider HERA [6, 7], where the well understood point-like electromagnetic interaction probes the parton structure in the diffractive reaction mechanism.

This has resulted in theoretical descriptions of data based on essentially two different approaches, one being pomeron exchange in Regge phenomenology and the other colour screening via soft gluon exchange in QCD.

The pomeron approach starts with the initial proton state fluctuating in a soft non-perturbative process into a proton and a pomeron. The latter is assumed to have a partonic structure which is probed by the momentum transfer Q^2 of the deep inelastic photon exchange to produce the hadronic final state, well separated in rapidity from the final state proton carrying most of the longitudinal momentum of the beam proton. HERA data on DDIS can then be described [3, 8] as a product of an effective pomeron flux factor from Regge phenomenology and deep inelastic scattering on the pomeron having parametrised parton density functions (PDF) [8]. Alternatively, one may parametrise diffractive structure functions without an explicit pomeron flux but instead being conditionally dependent on the momentum of the final proton.

However, this approach is not universal in the sense that such parametrisations do not reproduce diffractive hard scattering data in hadron-hadron collisions. For example, such pomeron PDFs overestimate substantially the cross-sections for diffractive hard scattering processes, such as production of jets or W, at the Tevatron [9]. This has called for introducing a gap survival suppression factor $\hat{S}$, which can be given a qualitative theoretical motivation but which is difficult to calculate quantitatively.

The colour exchange approach starts instead with the hard scattering process and then adds softer gluon exchanges to achieve the effective colour singlet exchange in diffractive processes. Thus, the underlying hard process is assumed to be the same as in the corresponding non-diffractive process and its momenta naturally not affected by other exchanges at much lower momentum transfer scales. However, the formation of confining colour fields may well be affected by the softer gluon exchanges and thereby the hadronisation process such that a different distribution of the final state hadrons emerges. For example, when different colour singlet string-fields emerge separated in rapidity they will hadronise into two hadron systems separated by a rapidity gap with no hadrons.

A simple, but phenomenologically rather successful model of this kind is the Soft Colour Interaction (SCI) model [10] added to the Lepto [11] and Pythia [12] Monte-Carlo event generators. A large variety of diffractive data could then be reproduced with essentially the same value of a single new parameter, introduced to give the probability for exchange a soft colour octet gluon between any pair of partons. This colour exchange alter the formation of the colour string-fields and hence the application of the conventional Lund string hadronisation model results in a different topology of the hadronic final state. The model gives an essentially correct description of diffractive DIS ep scattering at HERA [10] as well as diffractive events at the Tevatron having jets or quarkonia [13, 14] or gauge bosons [15]. It has therefore been applied for predictions, e.g. of diffractive Higgs production in double gap processes at LHC [16]. The gap survival factor $\hat{S}$ often used in other kinds of models, is not necessary here since the full event simulation accounts for such effects resulting in correct rates for the investigated diffractive processes in ep and pp and $p\bar{p}$ collisions.

Other models of a similar nature, with different forms of colour exchange, have been developed. The GAL model [17] for example considers soft colour exchanges between strings with a probability that favours minimization of the strings' area in energy-momentum coordinates. A recent development of such colour string reconnection models makes a more elaborate account for SU(3) colour statistics [18].

A theoretical QCD basis for basic colour exchanges has been proposed in [19] and, in a more elaborated form, in [20]. The basic hard scattering process is treated by conventional perturbative QCD (pQCD). Its large momentum scale implies that it occurs on a small space-time scale compared to the bound state proton and is thus embedded in the proton. Therefore, the emerging hard-scattered partons propagate through the proton's colour field and may interact with it. The amplitude for such multiple gluon exchanges is calculated in the eikonal approximation to all orders in perturbation theory resulting in an analytic expression for such a colour screening effect. It is this amplitude that we here develop into a probabilistic model. We implement it for two different Monte Carlo event generators: LEPTO for general deep inelastic lepton-nucleon scattering including first order QCD matrix elements and parton showers based on conventional $\log Q^2$ evolution from the DGLAP equations [21], and as well for CASCADE [22] specialised on small-x electron-proton scattering based on the off-shell $\gamma^\star g^\star \to q\bar{q}$ first order matrix element and $k_\perp$ factorisation with CCFM evolution [23] and unintegrated gluon density of the proton.

The paper is organized as follows. In section II we describe the basic process with the colour screening. Section III discusses the resulting cross-section for diffractive deep inelastic scattering and its Monte Carlo implementation. Section IV shows our results in comparison to HERA data. Finally, section V presents our conclusions.

II. SOFT COLOUR SCREENING IN DIFFRACTIVE DIS

In the virtue of the SCI model, the skeleton of both inclusive and diffractive (with rapidity gaps and/or leading proton) DIS process is provided by the same perturbative QCD diagram illustrated in Fig. 1. A parton with longitudinal momentum fraction x_P in the initial proton at the starting scale Q_0^2 for pQCD is evolved to smaller momentum fractions, but higher transverse momenta and virtualities up to a hard scale $\mu^2_{\rm hard} \simeq Q^2$. Here, a virtual photon γ^* with momentum q and virtuality $Q^2 = -q^2$ resolves a quark at Bjorken x

$$x = \frac{Q^2}{2P \cdot q} = \frac{Q^2}{Q^2 + W^2}\,. \tag{2.1}$$

At small x the process will dominantly be initiated by a gluon, which can radiate and splits into a $q\bar{q}$ pair. The total momentum fraction taken from the proton is $x_P = x/\beta$, and the total mass M_X of the parton system denoted as X in Fig. 1 is

$$M_X^2 = Q^2\left(\frac{1}{\beta} - 1\right) = Q^2\left(\frac{x_{\mathbb{P}}}{x} - 1\right)\,. \tag{2.2}$$

For a $\gamma g \to q\bar{q}$ pair (without additional gluons) having with quark transverse momentum $k_\perp$ and longitudinal momentum fraction z, the corresponding invariant mass is

$$M_X^2 = \frac{k_\perp^2 + m_q^2}{z(1-z)}\,. \tag{2.3}$$

At large x_P, the parton distribution functions (PDFs) of the incident proton are dominated by valence quarks leaving practically no chance for the proton to survive such an interaction, and hence resulting in a non-diffractive event. At small x_P, however, the PDFs are dominated by gluons, and the partonic system X is created in photon-gluon fusion $\gamma^* + g \to q\bar{q}$ as depicted in Fig. 1. In this case, the momentum exchange via multiple soft gluons with a small net fraction $x' \ll x_P$ between

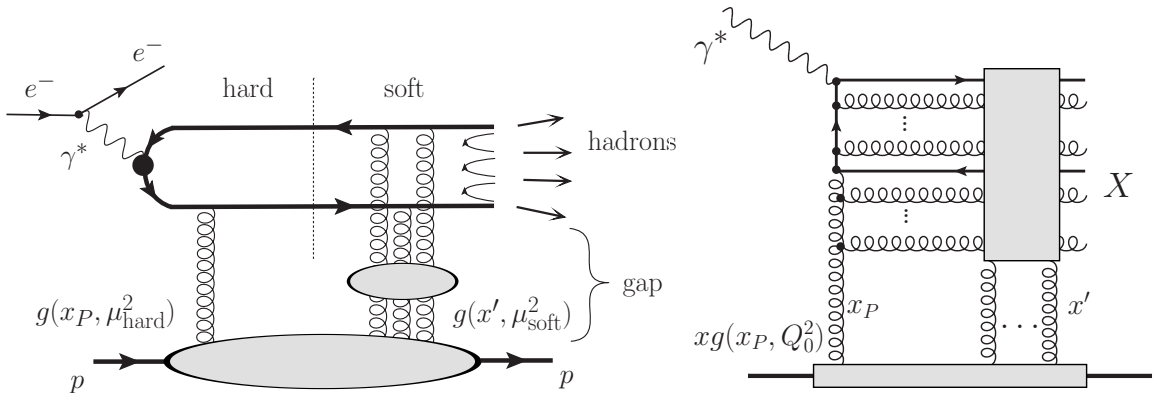

Figure 1. Illustration of the diffractive DIS process with the hard subprocess matrix element $\gamma^* g \to q\bar{q}$ with a subsequent rescattering of the $q\bar{q}$ dipole off the target colour field (left panel). Schematic diagram of the diffractive DIS process $\gamma^* p \to X + \mathrm{gap} + p$ accounting for final state rescattering by multiple gluon exchange at $x' \ll x_{\mathbb{P}}$ and perturbative parton shower off initial state parton which builds up the diffractive system X (right panel). The latter can be separated from the leading proton (or small-mass system Y) by a rapidity gap. The final state radiation is not shown as it does not affect the overall kinematics of the X system.

the proton and the perturbative X systems does not significantly change the momenta of partons emerging from the hard scattering. However, they do change the colour structure of the resulting X and Y systems.

The original SCI model captures the main effects in many processes as DDIS at HERA and diffractive hard scattering at the Tevatron. Despite this success, it is not derived from a perturbative QCD amplitude. For the case of DDIS, a derivation of the amplitude for the colour screened process has been done based on perturbative QCD in the large N_C limit [19, 20] and provides a theoretical basis for the DDIS process in terms of colour exchanges. It improves on the previous description by introducing a dependence on the kinematical details of the event which also leads to colour transparency. We start with the outline of the resummed colour screening amplitude and the derivation of probability for an event-by-event treatment in an event generator.

Consider the DDIS amplitude in impact parameter representation in the target rest frame which corresponds to the colour dipole picture of the process. The lowest Fock component of the virtual photon $\gamma^* \to q\bar{q}$ corresponds to its fluctuation to a $q\bar{q}$ dipole with transverse separation $\mathbf{r}$ in the colour background field of the traget proton at impact distance $\mathbf{b}$ from its centre. The prepared Fock component then propagates through the field in the proton and softly interacts with it such that it can, in principle, change its colour but not kinematics (the dipole size is frozen at the time scale of its propagation through the colour medium). We consider the forward limit where the total transverse momentum $\boldsymbol{\delta}_\perp$ of gluon exchanges in the t-channel is small, $|\boldsymbol{\delta}_\perp| \equiv \sqrt{-t} \simeq \mu_{\rm soft} \sim \Lambda_{\rm QCD}$. In this limit, as a straightforward consequence of the optical theorem in the limit of large $\gamma^* p$ c.m. energy, the DDIS amplitude $M_{\rm diff}$ can be written with the ordinary gluon-initiated inclusive DIS amplitude $M_g \equiv M_{g+\gamma\to X}$ and the dynamical colour screening (DCS) amplitude $\mathcal{A}_{\rm DCS}$ as

$$M_{\rm diff}(\mathbf{k}_\perp, \boldsymbol{\delta}_\perp) \propto \int d^2r d^2b\, M_g(x_P; \mathbf{r}, \mathbf{b})\, \mathcal{A}_{\rm DCS}(\mathbf{r}, \mathbf{b})\, e^{i\mathbf{r}\mathbf{k}_\perp} e^{i\mathbf{b}\boldsymbol{\delta}_\perp}\,,$$

where $\mathbf{k}_\perp$ is the relative quark transverse momentum in the $q\bar{q}$ dipole in the lowest order subprocess $g^* + \gamma^* \to q\bar{q}$.

The screening amplitude $\mathcal{A}_{\rm DCS}$ accounts for the soft gluon exchanges between the proton remnant Y and the rest of the final state commonly denoted as X, with $X = q\bar{q}$ at the lowest order. These exchanges carry a small longitudinal fraction x' and the transverse momentum transfer $k'_\perp$ is at a soft scale $\mu_{\rm soft}$. $\mathcal{A}_{\rm DCS}$ is resummed to all orders in the large-N_c limit where it acquires a simple eikonal

form [19, 20].

$$\mathcal{A}_{\rm DCS}(\mathbf{r},\mathbf{b}) = 1 - \exp\left(iC_F\alpha_s^{\rm eff}(\mu^2_{\rm soft})\,\ln\frac{|\mathbf{b}-\mathbf{r}|}{|\mathbf{b}|}\right) \tag{2.4}$$

Here, $C_F \simeq T_F N_c$ is the colour factor for the single gluon exchange amplitude and $\alpha_s^{\rm eff}$ is the effective coupling constant at the soft hadronic scale $\mu_{\rm soft}$. The effective QCD coupling is not small in this case. Several approaches dealing with the Landau singularities at low momentum transfers were proposed in the literature, e.g. [25]. In practice, we use the infrared-stable Analytic Perturbation Theory (APT) approach [26].

For our study we use similarly the inclusive amplitude

$$M_{\rm incl}(\mathbf{k}_\perp,\boldsymbol{\delta}_\perp) \propto \int d^2r d^2b\, M_g(x_{\mathbb{P}};\mathbf{r},\mathbf{b})\, e^{i\mathbf{r}\mathbf{k}_\perp} e^{i\mathbf{b}\boldsymbol{\delta}_\perp}\,. \tag{2.5}$$

In impact parameter space the fraction of the cross section with colour screening between the systems X and Y is obtained from the ratio

$$\frac{|M_{\rm diff}(\mathbf{r},\mathbf{b})|^2}{|M_{\rm incl}(\mathbf{r},\mathbf{b})|^2} = |\mathcal{A}_{\rm DCS}(\mathbf{r},\mathbf{b})|^2 \equiv P(\mathbf{r},\mathbf{b}) \tag{2.6}$$

which defines the probability function for the overall colour singlet exchange. With $\mathbf{rb} \equiv rb\cos\varphi$, this leads to

$$P(r/b,\varphi) = \left|1 - \exp\left(iC_F\alpha_s \ln\sqrt{1+\frac{r^2}{b^2}-2\frac{r}{b}\cos\varphi}\right)\right|^2\,. \tag{2.7}$$

To apply this as the probability in a Monte Carlo generated event at the parton level, we will associate $r \simeq \mathbf{k}_\perp^{-1}$ and $b \simeq \boldsymbol{\delta}_\perp^{-1}$, and approximate by taking the average over the relative angle φ

$$P(r/b) = \int \frac{d\varphi}{2\pi} P(r/b,\varphi) \tag{2.8}$$

which is motivated by the fact that φ will be uniformly distributed in a sample of many collisions. The result is shown in Fig. 2 for different choices of $\alpha_s^{\rm eff}$.

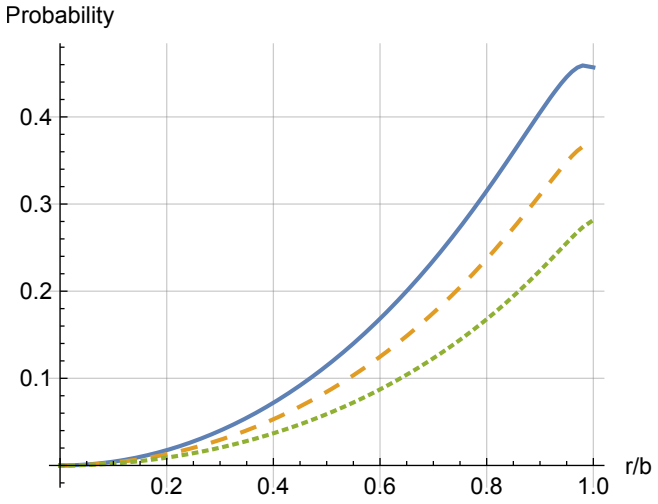

Figure 2. The screening probability $P(r/b)$ for different values of $\alpha_s^{\rm eff} \in \{0.7, 0.6, 0.5\}$ (upper to lower curve)

Its key characteristic property is infrared safety and the levelling off at large r/b resembling the saturation feature of the dipole scattering amplitude. Furthermore, the probability for the colour screening vanishes for small dipoles $r/b \ll 1$ which is compatible with the colour transparency property. We note that $\alpha_s^{\rm eff}$ enters the normalisation factor.

III. DDIS CROSS SECTION VIA DYNAMIC COLOUR SCREENING

The DDIS cross section is then obtained using the inclusive cross section and standard inclusive parton densities together with the probability $P(r/b)$ in Eq. (2.8) for dynamic colour screening resulting in

$$\frac{d\sigma^D}{dQ^2\,d\beta\,dx_P} = \sum_i \iint dx\,dr\,\rho(r,Q^2,\beta,x_P)\,\frac{d\hat{\sigma}}{dQ^2\,dx} \cdot f_i(x,Q^2)\,P(r/b)\,\delta(x-x_P\beta)$$

where $f_i(x,Q^2)$ are the standard inclusive parton distributions. $\rho(r,Q^2,\beta,x_P)$ represents the differential distribution of the standard DIS cross section in r which is obtained from the parton evolution event-by-event in the Monte Carlo. Since r represents the transverse size of the $q\bar{q}$ together with the pQCD radiation and the amplitude for colour screening is dominated by a rescattering off large dipoles, we use the smallest $k_\perp$ difference within the partonic X-system and let $r \simeq 1/k_{\perp\min}$. Although this $k_{\perp\min}$ is typically related to the pQCD cutoff, the Monte Carlo simulation can give very small such relative $k_\perp$ due to random angular orientations of the momentum vectors. We therefore introduce a cut-off $k_{\perp 0}$ to avoid a spurious divergence and transverse sizes r that are not perturbatively small. Thus we let $r = 1/\sqrt{k_{\perp\min}^2 + k_{\perp 0}^2}$.

The impact parameter $b \simeq 1/q_\perp$ is related to the soft transverse momentum of the screening multiple gluon exchange, which is expected to be well below the factorisation scale for the pQCD processes. On the other hand $q_\perp$ is expected to be somewhat larger than the confining energy-momentum scale $\Lambda_{\rm QCD} \sim 200\,\text{MeV}$ in order for the screening process to occur fast enough that the proton state can stay quantum mechanically coherent into the final state.

The colour screening probability therefore depends on the ratio r/b given by

$$\frac{r}{b} = \frac{q_\perp}{\sqrt{k_{\perp\min}^2 + k_{\perp 0}^2}}\,, \tag{3.1}$$

where $k_{\perp 0}$, as mentioned, regulates the divergence.

The values of $q_\perp$ and $k_{\perp 0}$ constitute the two free parameters of the model and are to be determined from a comparison with experimental data. From the construction, we expect their values to be approximately between $\Lambda_{\rm QCD}$ and the perturbative cutoff Q_0 in the gluon PDF. Using Eq. (3.1) in Eq. (2.8) results in a probability $P(k_{\perp\min})$ for the effective colour screening that depends on the internal kinematics of the system X.

We calculate the diffractive reduced cross section $\sigma_r^D(Q^2,\beta,x_P)$ within the same kinematic limits as applied by the experiment [27]. In addition, we adopt two different notions of the diffractive cross section. The first definition $\sigma_{r,\rm FWD}^D(Q^2,\beta,x_P)$ is based on a forward remnant system with a mass $M_Y < 1.6\,\text{GeV}$ and proton quantum numbers. The other definition $\sigma_{r,\rm LRG}^D(Q^2,\beta,x_P)$ requires a large rapidity gap (LRG) of two units in pseudorapidity. This choice is potentially sensitive to the inner radiation structure of the system X because the LRG is defined in terms of pseudorapidity.

A. Small-x resummation

The emissions in the CCFM evolution [23] are not strongly ordered in virtuality as they are by assumption in the DGLAP evolution [21]. Therefore, the parton in the hard interaction can no longer be approximated as on-shell and instead an off-shell matrix element is used for the hard interaction. Likewise, the branching gluons in the CCFM evolution are described by an unintegrated gluon density function (UGDF).

In the CCFM evolution, one effectively resums the leading logarithms in the energy splitting $1/z$ and $1/(1-z)$, as well as the leading logarithms in Q^2. Experimental data on the DDIS cross section $\sigma^D(Q^2,\beta,x_P)$ covers a wide kinematic range where one can have $M_X^2 \gg Q^2$. Because of

such potentially very different hard scales, we expect corrections from large logarithms to become important in certain parts of the phase space. Because of Eq. (2.2) we expect the CCFM evolution to be better suited for the DDIS observables, at least, in the case of $\beta \ll 1$ when the large leading logs

$$\ln \frac{M_X^2}{Q^2} \simeq -\ln \beta \gg 1$$

are properly treated.

B. Soft divergences

Because of the soft divergence in the first order QCD matrix element, the hard process $\gamma g \to q\bar{q}$ will favour an uneven splitting of the energy between the quarks. Specifically, if we define the fraction of energy taken by the quark as z, then the matrix elements have soft divergences as $1/z$ and $1/(1-z)$ for $z \to 0$ or $z \to 1$, respectively. One aspect of the soft divergence is that it favors a rather large ratio between x and the energy fraction x_n of the parton entering the matrix element. Specifically, in the matrix element $\gamma g \to q\bar{q}$ one can have a large ratio x/x_n without any additional radiation from the quark propagator. Such a large $\ln 1/z$ is not accounted for in the initial state parton evolution. In the case of the matrix elements $\gamma q \to q$ and $\gamma q \to qg$ plus DGLAP evolution this phase space is in part taken into account, but the DGLAP evolution does not resum potentially large $\ln x/x_n$.

Another aspect of the uneven splitting is that one of the quarks will be very forward in pseudo-rapidity in the lab frame when z is close to the divergence. In this case, the quark can have a large enough forward momentum p_z to populate the gap region and the event therefore does not contribute to the diffractive cross section as defined in terms of a LRG in spite of having a leading proton.

The divergent behaviour is unphysical and is usually avoided with a cutoff. Still, an inclusion of higher order effects may be important for the cross section and also for the inner structure within the X system. In particular, the energy of the $q\bar{q}$ system may be shared by additional gluons and therefore significantly reduce the rapidity range of the final X-system and therefore can have an influence on the LRG observable.

C. Details of the Monte Carlo implementation

In order to study the dynamic colour screening in more detail, we interface the model with different Monte Carlo event generators. In particular, we employ the program LEPTO [11] which offers first order QED and first order QCD matrix elements combined with DGLAP [21] parton showering and collinear PDFs. As a second program we use CASCADE [22] which offers $\gamma^* + g^* \to q\bar{q}$ with $k_\perp$-factorised off-shell matrix elements and CCFM evolution [23] which is intended to account for potentially large logarithms of incident momentum fractions of radiated partons. The photon-gluon fusion matrix element $\gamma + g \to q\bar{q}$ illustrated also in Fig. 1 is the dominant contribution to the diffractive DIS cross section at small x. LEPTO includes this process as a first order QCD matrix element, as well as via a combination of the QED hard process $\gamma^* q \to q$ augmented by a $g \to q\bar{q}$ DGLAP splitting. CASCADE provides this process as an off-shell first order QCD matrix element, but not as a first order QED matrix element with parton splitting.

After generating events on parton level using matrix elements augmented with initial and final state parton showers, we apply the colour screening model before any special treatment of the remnant. In particular, we do not allow any cluster fragmentation of systems with a small invariant mass because the dynamic screening will potentially change the colour topology of the event before the scale of hadronization is reached and therefore change the possible outcomes of the fragmentation. This is understood as colour rescattering to happen on the scale between the perturbative cutoff at $\sim 1\,\mathrm{GeV}$ and Λ_{QCD} of hadronisation.

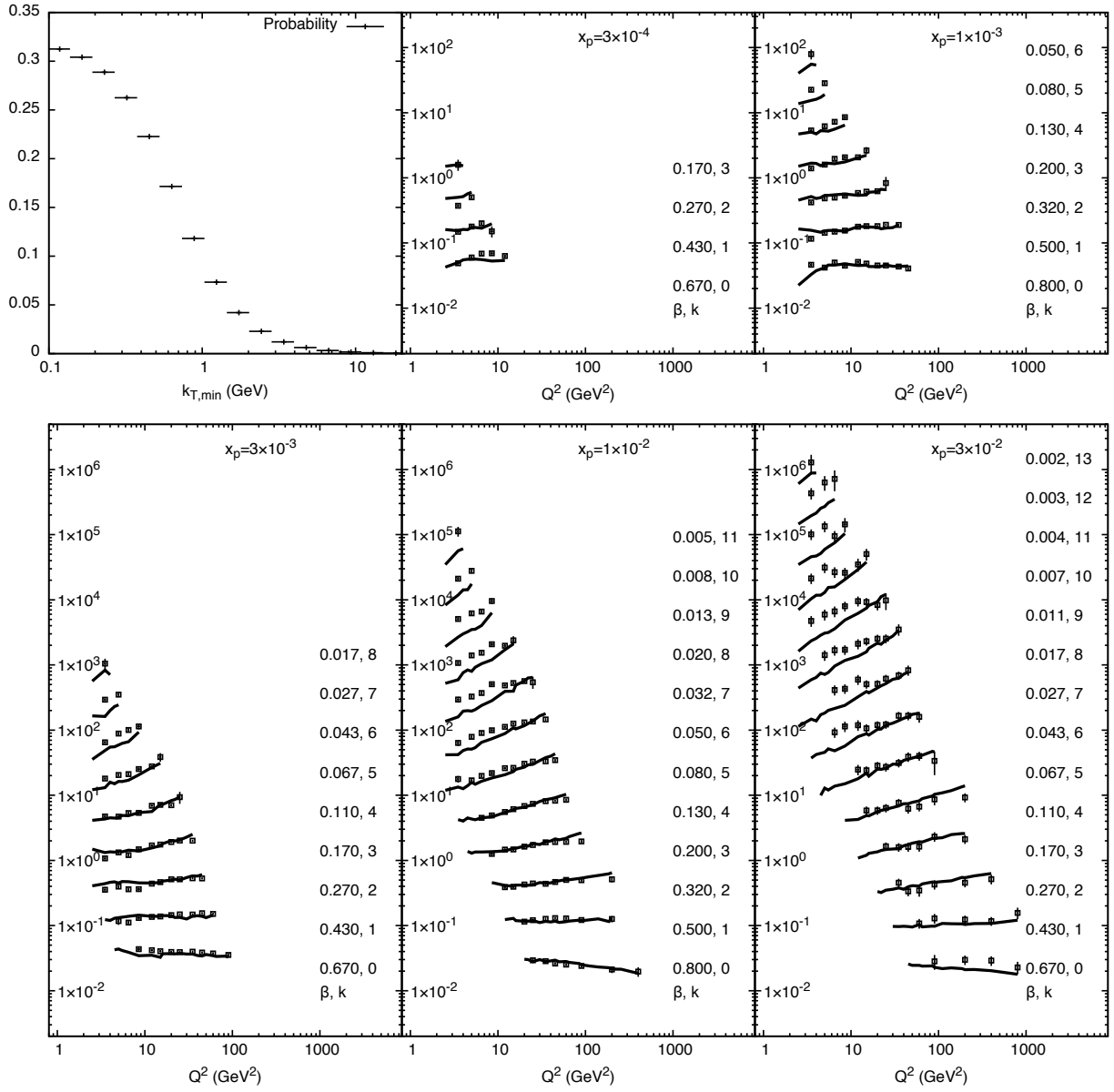

Figure 3. The reduced diffractive cross section $\sigma^D(Q^2, \beta, x_P)$ in comparison with the H1 data [27]. The model prediction uses dynamic colour screening with the parameters $k_{\perp 0} = 0.72\,\text{GeV}$ and $q_\perp = 0.58\,\text{GeV}$ and the CASCADE event generator with CCFM evolution. $P(k_{\perp\text{min}})$ for the fitted parameters is shown in the upper-left corner. Diffractive events in the model are defined as having a remnant system Y with proton quantum numbers and invariant mass $M_Y < 1.6\,\text{GeV}$. Rows for different values of β are offset by a factor 3^k as indicated on the figure.

The remnant system is in a Monte Carlo program treated by a non-perturbative model. For the case that the perturbative interaction resolves a gluon, which is the class of events which potentially leads to diffraction, the remnant is usually split into a (qq, q) pair with a certain sharing of momenta. This splitting typically introduces a relative transverse momentum representing the Fermi motion in the bound state proton which is given by a Gaussian distribution with a width $\sim \Lambda_{\text{QCD}}$. This relative $k_\perp$ affects the later hadronisation which introduces an uncertainty for the prediction of a forward proton spectrum. In this work, we are interested in diffraction defined by a forward small-mass system with proton quantum numbers or a large rapidity gap, which is insensitive to whether the hadronisation model maps the small-mass forward remnant state to a proton state or a resonance.

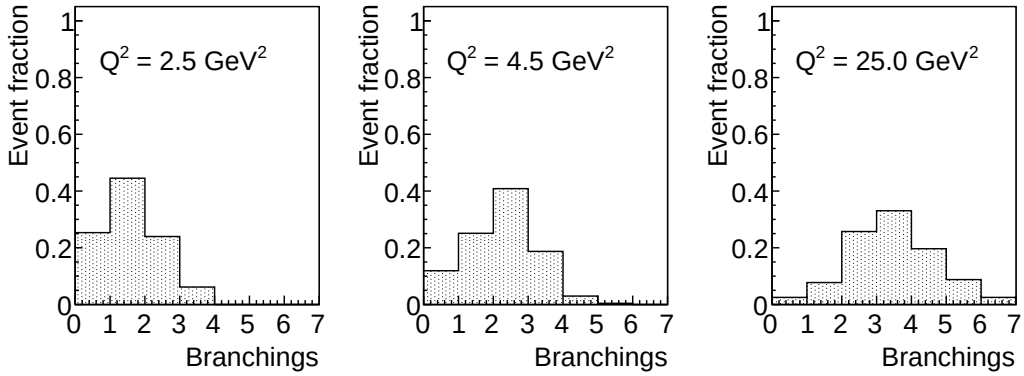

Figure 4. The distribution of the number of initial state radiation branchings in the CCFM evolution at $x_P = 3 \times 10^{-2}$, $\beta = 0.017$ and for different values of Q^2. As the hard scale increases, there is more phase space for initial state radiation available and we see more gluon branchings. As the number of gluon branchings increases, a larger part of the full perturbative event and specifically its β-value is described using CCFM evolution which leads to a more accurate differential cross section.

All plots of the diffractive cross section in this paper show the reduced cross section σ_r which is related to the cross section via

$$\frac{d\sigma}{dQ^2\, d\beta\, dx_P} = \frac{4\pi\alpha_{EM}^2}{\beta Q^4}\left(1 - y + \frac{y^2}{2}\right)\sigma_r(Q^2, \beta, x_P)$$

with y given as

$$y = \frac{Q^2}{x(s - m_N^2)} \simeq \frac{Q^2}{xs}$$

with the negligible nucleon mass m_N.

IV. RESULTS

A. Dynamic colour screening

Fig. 3 shows the diffractive cross section $\sigma_{r,\mathrm{FWD}}^D$ obtained with dynamic colour screening and the process $\gamma^* g^* \to q\bar{q}$ from the CASCADE event generator with CCFM evolution. Events are selected according to the forward small-mass system prescription which requires a remnant system Y with proton quantum numbers and invariant mass $M_Y < 1.6\,\mathrm{GeV}$. The two parameters of the rescattering model are fitted and we obtain $k_{\perp 0} = 0.72\,\mathrm{GeV}$ and $q_\perp = 0.58\,\mathrm{GeV}$. These values are physically reasonable in the sense that both are between Λ_{QCD} and Q_0, and that the typical transverse size of the proton background $q_\perp$ is smaller than the minimal transverse scale $k_{\perp 0}$ of the partonic X system.

We note that there is an overall good agreement with experimental data over a very wide region of the kinematical space. This agreement is remarkable because the model does not introduce specialised diffractive parton distributions, but uses standard proton UGDFs as input and introduces only two new physically motivated parameters.

Nevertheless, we note that some kinematic regions are not very well described. The deviations from the data can be correlated with the kinematic region where β and Q^2 are small, as well as x_P is large. This can be partly understood from the parton evolution. At small β, meaning large M_X^2 compared to Q^2, large logarithms of $1/\beta$ become important. On the other hand, at small Q^2 scales, the event is mainly described by the matrix element, whereas the shower activity is low, which leads to a relative damping of the cross section with respect to the data. The effect of low radiative activity is illustrated in Fig. 4 where we show the number of branchings in the evolution at a representative

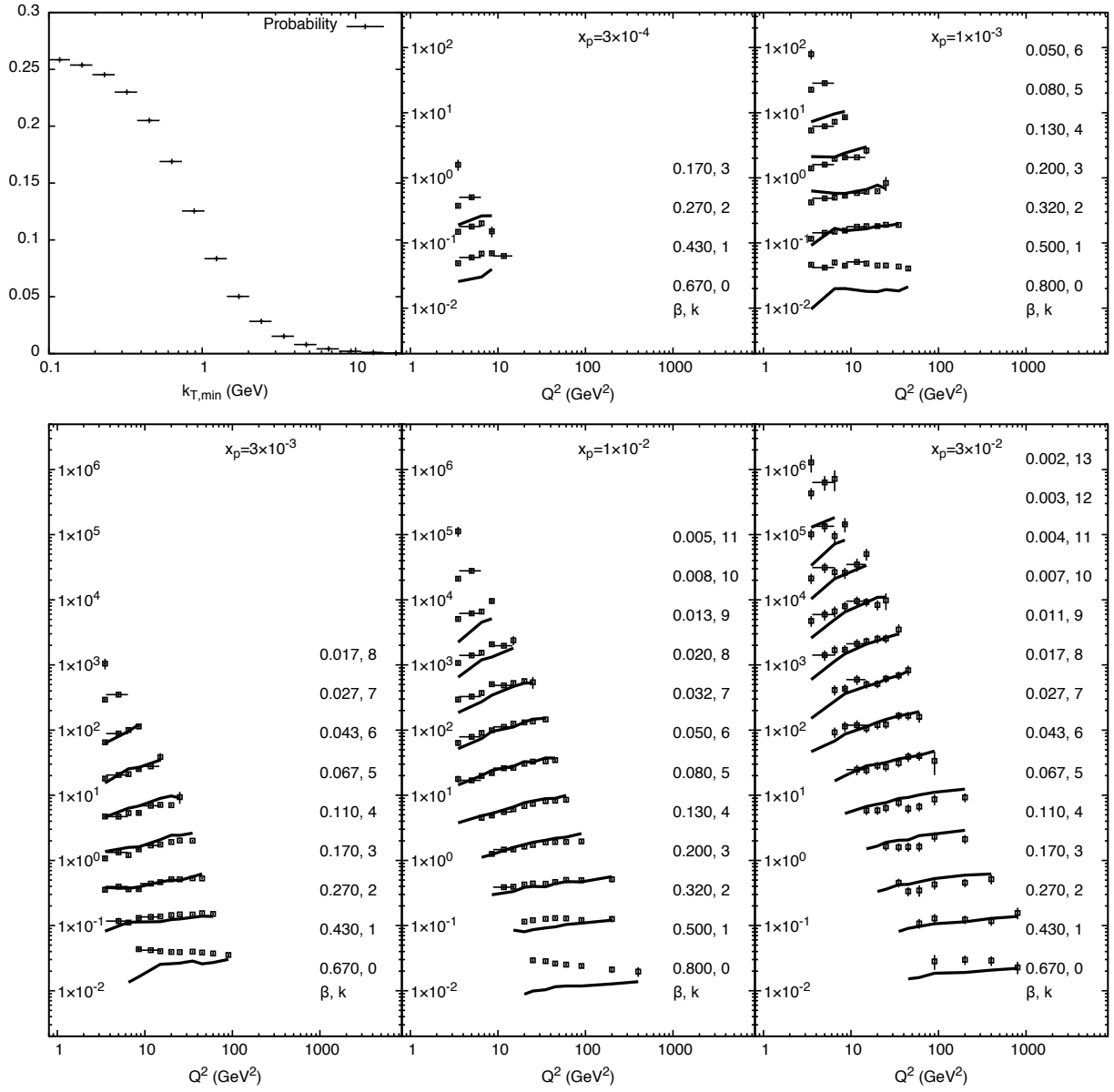

Figure 5. The reduced diffractive cross section $\sigma^D(Q^2, \beta, x_P)$ as in Fig. 3 but using the LEPTO event generator with DGLAP evolution. The parameters for the dynamic colour screening model obtained from the fit against data [27] are $k_{\perp 0} = 0.89\,\text{GeV}$ and $q_\perp = 0.66\,\text{GeV}$.

value of $\beta = 0.017$ for different Q^2. In the region of large x_P, one could be sensitive as well to the contribution from intermediate quarks which is not treated in the CCFM evolution.

We compare the result of the CASCADE simulation with that of LEPTO shown in Fig. 5. The corresponding parameters obtained for the dynamic colour screening model are $k_{\perp 0} = 0.89\,\text{GeV}$ and $q_\perp = 0.66\,\text{GeV}$. We note that the description is good in the inner region of the kinematic space. At very small β though, the description is significantly worse than the corresponding result in Fig. 3, which is the region where one expects large corrections from logarithms in $1/\beta$. Still, we note that the results from LEPTO agree with data slightly better in the region of large x_P, small Q^2 and intermediate β. This can be understood in terms of the different parton evolution methods because a part of the cross section in this region is described in LEPTO by the first order QED process with parton evolution and incorporates the leading resummation of the quark line before it couples to the virtual photon.

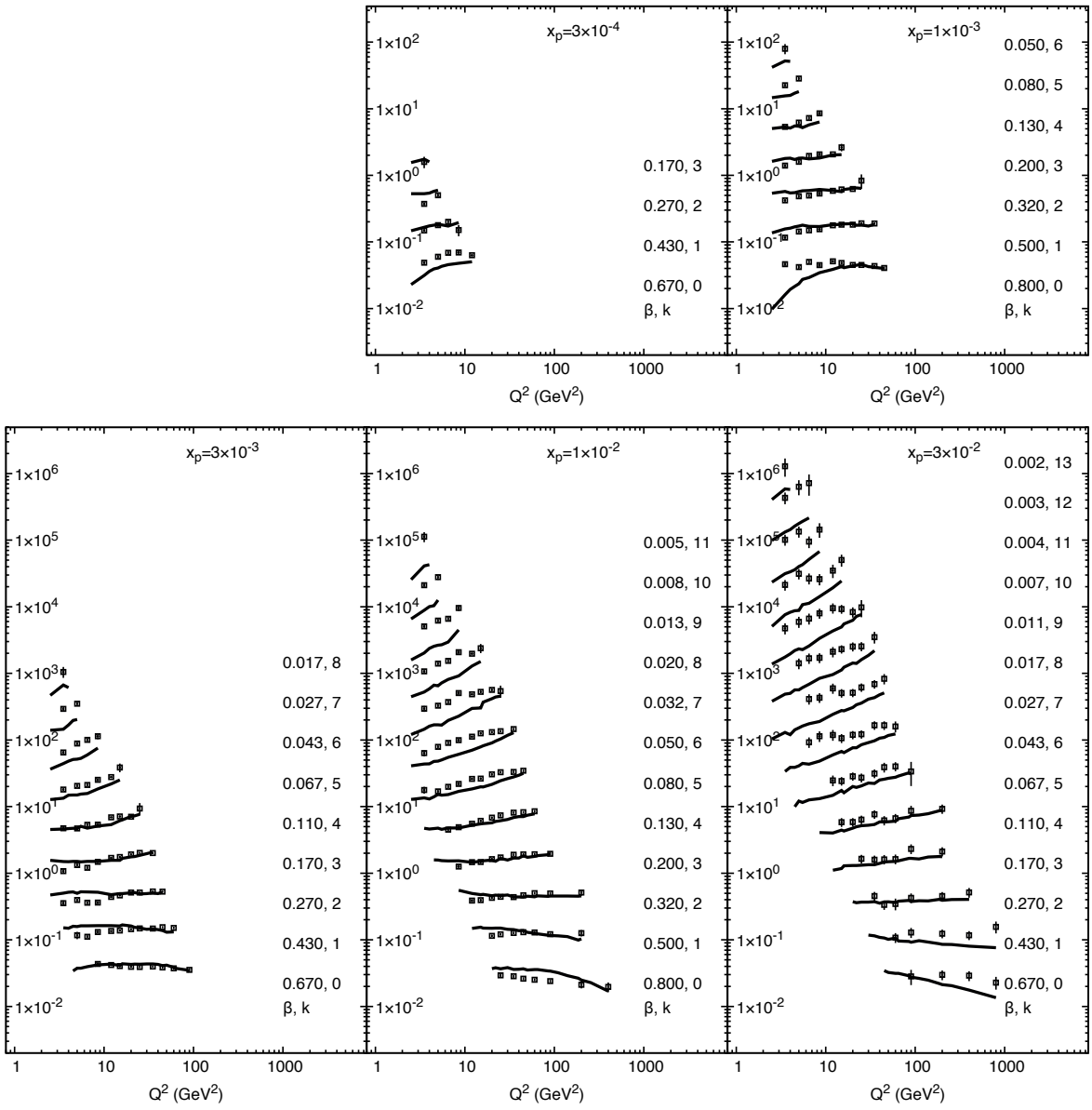

Figure 6. As in Fig. 3 but with a constant probability of $P = 0.103$ fitted from this data. We observe that especially at small β the resulting diffractive cross section has a significantly different slope with respect to Q^2 and the description of data is not as good as in the case of the dynamic rescattering model.

B. Colour screening probability

It is interesting to compare the dynamic colour screening model with the results from having a fixed colour screening probability while keeping all other parameters equal. Fig. 6 shows the diffractive cross section with $P = 0.103$, obtained by a fit to data. We note that the constant probability results in a significantly worse description of the data. The overall normalisation as well as the shape of $\sigma^D(Q^2, \beta, x_P)$ with respect to Q^2 is better described by the dynamic screening model.

In the results from the dynamic model of Fig. 3, we have fitted the two parameters $k_{\perp 0}$ and $q_\perp$ of the dynamic screening model to data. The parameters determine the overall normalisation and essentially the position of the slope where the screening probability $P(k_{\perp\min})$ falls off to zero. On the other hand, the general shape of this probability is given by the underlying model itself. It is interesting though to investigate what form of $P(k_{\perp\min})$ would result in a good fit without assuming

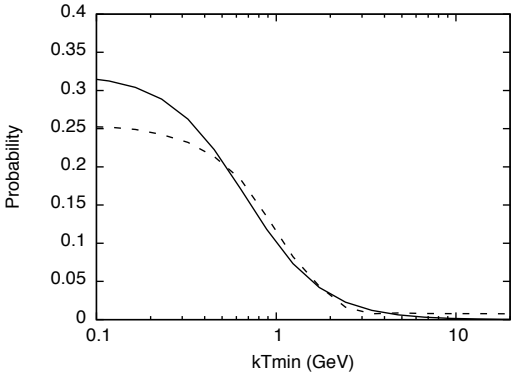

Figure 7. Dashed line: The fit of a free-form probability function $P(k_{\perp\min})$ constrained only by the requirement to be in the physically sensible range $[0, 1]$ and to be fairly smooth. Solid line: The probability from the fit of the colour screening model as used in Fig. 3 (upper left corner). We note that both methods result in very similar functions for $P(k_{\perp\min})$.

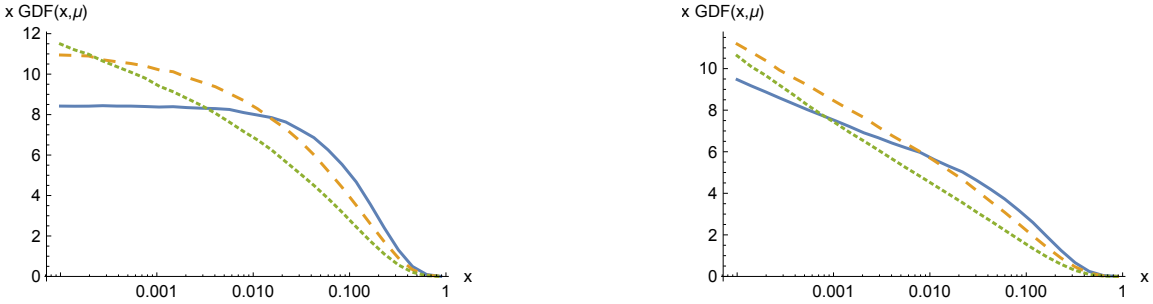

Figure 8. The gluon density A0 from CASCADE [22] integrated over $k_\perp$ at the scales 1, 4 and 8 GeV for the solid, dashed and dotted lines, respectively, is shown in the left panel. The gluon density A1 for the same scales is shown in the right panel. The distribution starts out with a steeper slope at small scales and influences the observable as shown in Fig. 9.

an underlying model. To this end, we fit a mapping $k_{\perp\min} \to P$ which is only constrained by the fact that it should lie in the physically sensible range [0, 1] and that it should be reasonably smooth. The result of such a fit is shown in Fig. 7. We observe that even though we did not place any particular constraints on the functional form, both methods yield function with a very similar shape which supports prediction by the dynamic screening model.

C. Dependence on the gluon density

The result in Fig. 3 is obtained using the unintegrated gluon density $xA(x, k_\perp^2, \mu)$ illustrated in Fig. 8 (left). This density starts out flat at a low scale μ which can be compared with the $1/x_P$ behavior of the pomeron flux in Regge-based models. The diffractive cross section in our model is sensitive to the slope especially in the kinematic region where β is large. We can compare the main result in Fig. 3 with the result obtained by using a parton density which has a stronger increase towards small x already at low scales, shown in Fig. 8 (right). The corresponding $\sigma^D_{r,\mathrm{FWD}}$ is shown in Fig. 9. We note that especially the dependence of the cross section on Q^2 is sensitive to the gluon density $xA(x, k_\perp^2, \mu)$ at small scales μ. By including diffractive data into the fit of a gluon density, this dependence could be used to further constrain the shape of the gluon distribution at low scales.

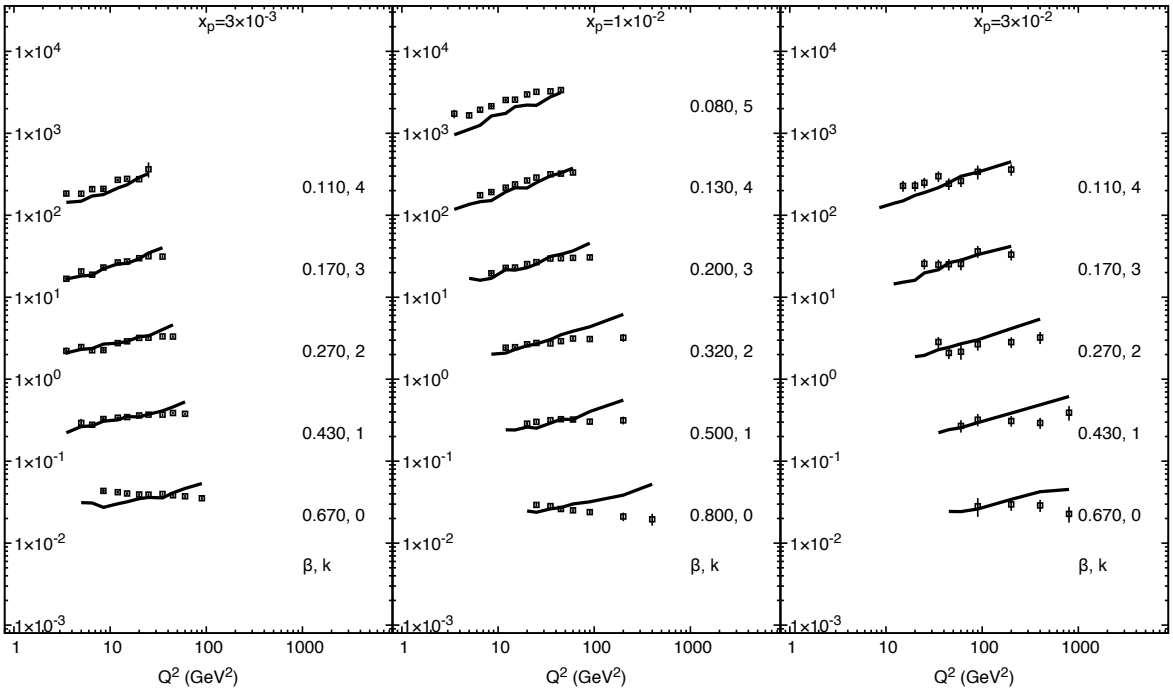

Figure 9. As in Fig. 3 but using a gluon density $xA(x, k_\perp, \mu)$ that increases stronger towards low-x already at the starting scale (A0 in [22]). Only the interesting subset of the kinematic plane is shown. By comparison with Fig. 3 it is seen that $\sigma^D(Q^2, \beta, x_P)$ is at large β and large x_P sensitive to the shape of the gluon density at the starting scale.

D. Diffractive cross section with a large rapidity gap

The diffractive cross section $\sigma^D_{\rm LRG}(Q^2, \beta, x_P)$ as defined by the presence of a LRG in the event depends additionally on the internal details of the system X. While the remnant is well forward and separated from the LRG region in pseudorapidity, the final states of the X system can have a momentum that points into the LRG even though the event was mediated by an effective colour-singlet exchange. This observable is therefore not only sensitive to the overall β of the event, but also to the kinematic distribution of the hard interaction and the parton showers. Fig. 10 shows $\sigma^D_{\rm LRG}(Q^2, \beta, x_P)$ for a LRG in the range $[4 \ldots 6]$ in pseudorapidity. We note a quite good agreement and similarity to Fig. 3.

We expect $\sigma^D_{\rm LRG}(Q^2, \beta, x_P)$ to be sensitive to higher order corrections. Especially the part of the cross section close to the soft divergence $1/z$ contributes to the set of events which produce activity in the LRG region and therefore cause a difference from the $\sigma^D_{\rm FWD}(Q^2, \beta, x_P)$ defined by the forward-system definition. This is illustrated in Fig. 11 where the fraction of q and g with a momentum in the LRG is shown. We note that the fraction of quarks in the LRG increases towards low Q^2 which can be understood from the correlation between Q^2 and the transverse momentum. On the other hand, the fraction of gluons in the LRG depends more strongly on x_P and weaker on Q^2. This can be understood from the fact that gluons arise from the parton shower in contrast to the quarks which are defined by the matrix element.

At the leading order of our computation, we note that the result is only mildly sensitive to the cuts employed to regulate the $1/z$ divergence. Also, a comparison with massive matrix elements at leading order suggests that typical quark masses lead effectively to the cuts on the energy sharing variable z as used in our results. On the other hand, higher order corrections could significantly alter the internal event structure, especially in the region of the phase space where it is likely to have a large step z between x and x_n. There, an additional final state gluon could modify the extension of the X system in rapidity. An improved parton evolution based on CCFM with additional splittings

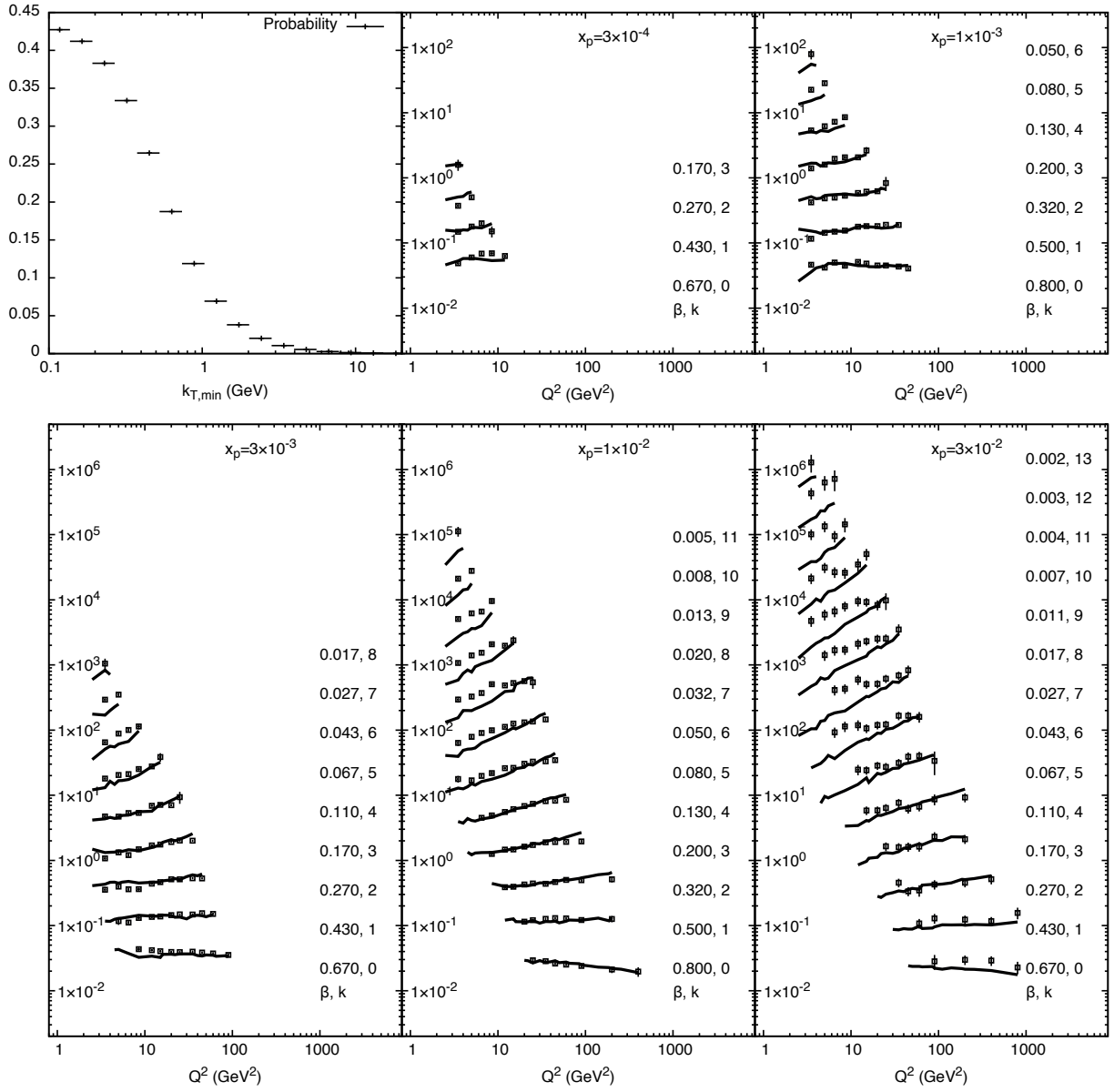

Figure 10. As in Fig. 3 but showing $\sigma^D_{r,\mathrm{LRG}}$ where the diffractive cross section is defined in terms of a large rapidity gap between $\eta_{min} = 4.0$ and $\eta_{max} = 6.0$ in pseudorapidity.

$g \to qq$ and $q \to qg$ could therefore in principle improve the description further because the diffractive process at a low scale could be described with a QED matrix element and low x resummed parton evolution. Similarly, $\sigma^D_{\mathrm{LRG}}(Q^2, \beta, x_P)$ is also sensitive to the distribution of the transverse momenta and energy splitting in the parton shower.

V. SUMMARY AND CONCLUSIONS

We have developed the probablity for dynamic colour screening in DIS in a way that can be used in Monte Carlo event generators and applied it with CASCADE and LEPTO. The resulting model predicts the diffractive DIS cross section based on perturbative QCD matrix elements and standard inclusive parton densities in both collinear and $k_\perp$-factorisation approaches. This facilitates practical applications of previously obtained theoretical derivations of the amplitude for colour screening

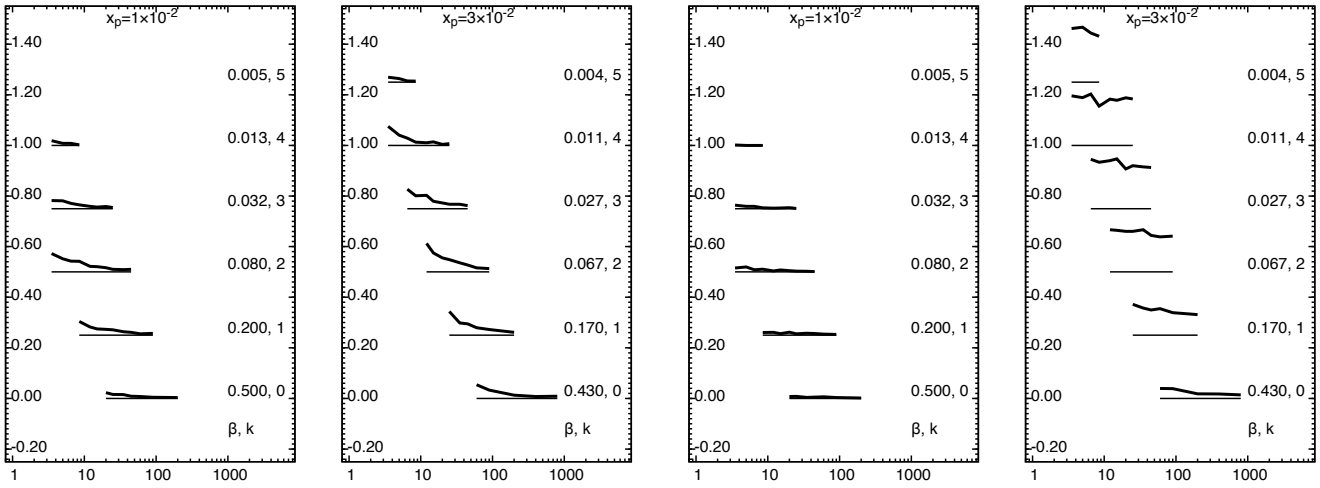

Figure 11. The fraction of events with a parton level quark with a pseudorapidity in the gap region is shown in the two leftmost plots. The 0% level within the Q^2 range available in the experimental data is indicated by a horizontal thinner line for each row in β. The fraction of events with a gluon in the LRG region is shown in the two rightmost plots.

through semi-soft multiple gluon exchanges calculated in the eikonal approximation to all orders in perturbative QCD. The basic formalism gives a theoretical understanding why the phenomenologically soft colour interaction (SCI) model has been phenomenologically successful, but goes beyond that model by leading to a colour screening probability that depends on the dynamics of the perturbative QCD parton dynamics. This dynamical screening probability exhibits a saturated shape at small transverse momenta of the emerging parton system as well as colour transparency at large transverse momentum.

The Monte Carlo model has only two, physically motivated parameters. Their values are obtained by fitting the HERA diffractive cross section and found to be of the expected magnitude. The model successfully describes the data over a large kinematic range, significantly better than with a constant screening probability. Interestingly, a fit of a free-form probability function results in the same shape as our model, and hence gives support for our account of the basic QCD dynamics of relevance.

In some kinematic regions there are two very different scales present, namely the invariant mass of the diffractive system M_X^2 and the photon virtuality Q^2. This calls for a resummation of large logarithms $\log M_X^2/Q^2$, or equivalently $\log 1/\beta$. To address this issue, we take the cross section in the $k_\perp$-factorisation approach from off-shell matrix elements and unintegrated gluon densities together with the CCFM evolution which provides a resummation of leading logarithms in $1/x$. We show that this significantly improves the description of the diffractive HERA data at $\beta \ll 1$ corresponding to $M_X^2 \gg Q^2$. Nevertheless, there are residual deviations in the region where both β and Q^2 are at their lowest values. This may be attributed to the extreme region of very small z when the quark propagator connected to the virtual photon have a significant phase space available for gluon radiation, which is not accounted for; neither in the leading order matrix element for $\gamma^\star g^\star \to q\bar{q}$ nor in the CCFM evolution that does not include the $q \to qg$ splitting. The DGLAP evolution does include this and also shows a slightly better result in this case, but is still not sufficient since here the effects of large $\log 1/x$ is not included.

To conclude and connect to the discussion in the Introduction, our study has shown that the phenomenon of diffractive deep inelastic scattering can be described using a basic QCD-framework. The hard subprocess is treated in the same way as for non-diffractive events but a colour screening process occurs as a result of multiple gluon exchanges that are resummed to all orders. Significant deviations from data occur in a special kinematic region, where potentially large logarithmic corrections are not yet fully included in available evolution equations for gluon radiation. Still, the overall results show that gluonic colour screening in QCD seems to be a viable approach to understand diffraction.

Acknowledgments This work was supported by the Swedish Research Council under contracts 621-2011-5107 and 621-2013-4287.

---

[1] J. C. Polkinghorne, Cambridge, Uk: Univ.Pr.(1980) 131p
[2] J. R. Forshaw and D. A. Ross, Cambridge Lect. Notes Phys. **9**, 1 (1997).
[3] G. Ingelman and P. E. Schlein, Phys. Lett. B **152**, 256 (1985).
[4] R. Bonino *et al.* [UA8 Collaboration], Phys. Lett. B **211**, 239 (1988).
[5] G. Ingelman, Int. J. Mod. Phys. A **21**, 1805 (2006) [hep-ph/0512146].
[6] S. Chekanov *et al.* [ZEUS Collaboration], Nucl. Phys. B **816**, 1 (2009); T. Ahmed *et al.*, Nucl. Phys. B **429**, 477 (1994); Nucl. Phys. B **435**, 3 (1995).
[7] F. D. Aaron *et al.* [H1 and ZEUS Collaborations], Eur. Phys. J. C **72**, 2175 (2012) [arXiv:1207.4864 [hep-ex]].
[8] G. Ingelman and K. Prytz, Z. Phys. C **58**, 285 (1993).
[9] T. Affolder *et al.* [CDF Collaboration], Phys. Rev. Lett. **84**, 5043 (2000).
[10] A. Edin, G. Ingelman and J. Rathsman, Phys. Lett. B **366**, 371 (1996); Z. Phys. C **75**, 57 (1997).
[11] G. Ingelman, A. Edin and J. Rathsman, Comput. Phys. Commun. **101**, 108 (1997).
[12] T. Sjöstrand, S. Mrenna and P. Z. Skands, JHEP **0605**, 026 (2006) [hep-ph/0603175].
[13] A. Edin, G. Ingelman and J. Rathsman, Phys. Rev. D **56**, 7317 (1997).
[14] R. Enberg, G. Ingelman and N. Timneanu, Phys. Rev. D **64**, 114015 (2001).
[15] G. Ingelman, R. Pasechnik, J. Rathsman and D. Werder, Phys. Rev. D **87**, no. 9, 094017 (2013) [arXiv:1210.5976 [hep-ph]].
[16] R. Enberg, G. Ingelman, A. Kissavos and N. Timneanu, Phys. Rev. Lett. **89**, 081801 (2002).
[17] J. Rathsman, Phys. Lett. B **452**, 364 (1999) [hep-ph/9812423].
[18] J. R. Christiansen and P. Z. Skands, JHEP **1508**, 003 (2015) [arXiv:1505.01681 [hep-ph]].
[19] S. J. Brodsky, R. Enberg, P. Hoyer and G. Ingelman, Phys. Rev. D **71**, 074020 (2005).
[20] R. Pasechnik, R. Enberg and G. Ingelman, Phys. Rev. D **82**, 054036 (2010); Phys. Lett. B **695**, 189 (2011).
[21] V. N. Gribov and L. N. Lipatov, Sov. J. Nucl. Phys. **15**, 438 (1972) [Yad. Fiz. **15**, 781 (1972)];
G. Altarelli and G. Parisi, Nucl. Phys. B **126**, 298 (1977);
Y. L. Dokshitzer, Sov. Phys. JETP **46**, 641 (1977) [Zh. Eksp. Teor. Fiz. **73**, 1216 (1977)].
[22] H. Jung and G. P. Salam, Eur. Phys. J. C **19**, 351 (2001) [hep-ph/0012143].
[23] S. Catani, F. Fiorani and G. Marchesini, Nucl. Phys. B **336**, 18 (1990);
S. Catani, F. Fiorani and G. Marchesini, Phys. Lett. B **234**, 339 (1990);
S. Catani, M. Ciafaloni and F. Hautmann, Nucl. Phys. B **366**, 135 (1991);
G. Marchesini, Nucl. Phys. B **445**, 49 (1995) [hep-ph/9412327].
[24] B. Andersson, G. Gustafson, G. Ingelman and T. Sjöstrand, Phys. Rept. **97**, 31 (1983).
[25] S. J. Brodsky, G. F. de Teramond and A. Deur, Phys. Rev. D **81**, 096010 (2010).
[26] D. V. Shirkov and I. L. Solovtsov, Phys. Rev. Lett. **79**, 1209 (1997).
[27] F. D. Aaron *et al.* [H1 Collaboration], Eur. Phys. J. C **72** (2012) 2074 [arXiv:1203.4495 [hep-ex]].